Chapter I

Growth and first characterization of Cr-doped CdTe quantum dots

During this thesis, we studied two types of magnetic quantum dots: self assembled QDs and strain free QDs. The self assembled are formed by the partial relaxation of the strain of a CdTe layer on a ZnTe substrate (Stranski-Krastanov dots). Strain free dots are formed by thickness variation of a CdTe /CdMgTe thin quantum well. The growth of Cr doped samples were done in Pr. Shinji Kuroda laboratory, in the University of Tsukuba. The Mn-doped samples were grown at Grenoble, in the CEA-CNRS joined team NPSC, by Dr. Hervé Boukari.

We will focus in this chapter on the growth done at Tsukuba by Molecular Beam Epitaxy (MBE). We begin by giving some general explanation on the MBE process and the different tools that are used in it. We then go to the growth of the self-assembled Cr-doped quantum dots, detailing the preparation of the substrate, the growth, and discussing the first characterization of the samples. In the last section, we present two other kinds of sample we grew: samples with the possibility of applying an electric field on them, and the strain free dots. For each of them, we detail the growth process and present basic characterization.

I.1 The Molecular Beam Expitaxy

The samples we used are grown using epitaxy. It consists on depositing atoms or molecules on the surface of the sample. Each elements are deposited on top of each other, and the lattice parameter of the substrate in the plane is kept as long as no defect appears in the material. The elements condensate on the surface, where they can diffuse before getting adsorbed, or re-evaporate in the gas. The substrate temperature is tuned in order to maximise the mobility of the elements, to get a flat surface, while minimizing the re-evaporation. To achieve such a growth, we

used a process called Molecular Beam Epitaxy (MBE), in which flux of elements are evaporated toward the sample, where each atom or molecule is deposited and crystallize. This is done using cells of elements heated to control their evaporation or until they reach sublimation.

The MBE process was first devised at the end of the 1960s [1]. This method offers a good control on the growth, which make it useful for the development of nanostructures. Depositing the materials layer by layer gives the possibility to grow really thin structure, and the transition between two materials can be made really abrupt, with the possibility to go from one material to another over a single monolayer (ML).

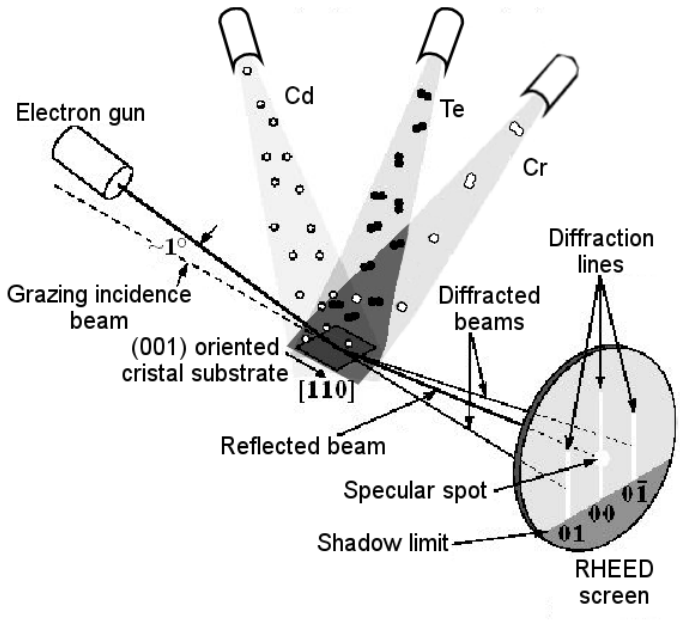

Figure I.1: Schema of a MBE cells and substrate during a growth. An electron gun is attached to the chamber in order to probe the surface of the sample.

The elements are kept in Knudsen cells, which consist of a crucibles of high-melting-point material wrapped in Tungsten filament acting as heater. A shutter is put in front of them to stop the element flux. During the growth, the shutter is opened to let the element travel to the substrate. The growth by MBE is a slow process: it can takes more than a hour to get a layer 1 μm thick. In order to avoid contamination, Ultra High Vacuum, in the order of 10^{-8} Pa, is needed. Under this condition, the mean free path of the gas is long compared to distance to the sample (km for the mean free path of gas, when the distance between the substrate and the cell is of the order of 50 cm). This process is illustrated in Fig. I.1. Reaching the

surface, the atoms diffuse before stopping, either having dissipated their kinetic energy through interaction with the surface, or (more commonly) being kept by islands steps created by previously deposited atoms. The growth occur layer by layer, slowly (about 1 ML/s), giving a good control of the thickness of the grown material.

The growth can be monitored in-situ with RHEED (Reflexion High-Energy Electron Diffraction). An electron gun send a beam of high energy electrons, extracted from a filament by high bias voltage, at a low angle, between 1° and 3°, to the surface sample. This way, the electrons will only probe the surface of the sample, penetrating the material only on a few MLs. From the difracted pattern, we can get information on the morphology of the surface. We can also use the variation of intensity of the specular spot, the spot at lowest angle reflected, to measure the growth rate of the deposited material, as illustrated on Fig. I.2.

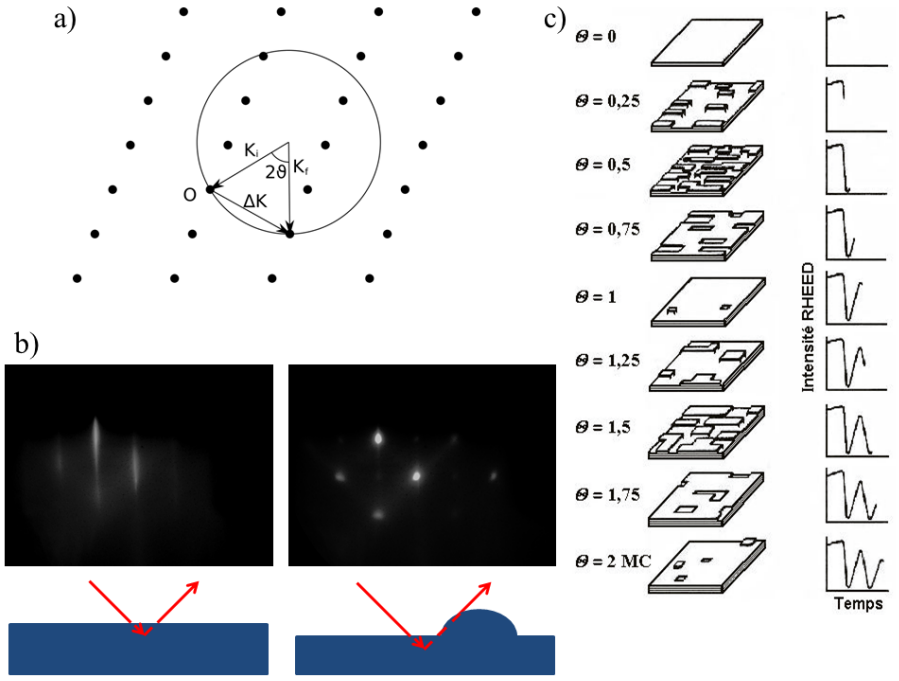

Figure I.2: (a) Construction of the Ewald sphere in the reciprocal space for an elastic scattering. For diffraction to occur, the reciprocal lattice must lie on the Ewald sphere. (b) Change of the RHEED pattern from a flat surface (left) to a rough one due to the formation of QDs (right). (c) Surface state during the growth of 2 MLs (left) and RHEED intensity for each step (right).

Incident electrons have a wave vector $\mathbf{k_i} = 2\pi/\lambda_e$, with λ_e the electron wavelength, typically 30 or 40 pm for an electrons at 30-40 keV. Since only scattered

diffraction is considered, the diffracted wave vector $\mathbf{k_f}$ as the same module as the incident one $\mathbf{k_i}$. The Ewald's sphere has then a radius equal to $||\mathbf{k_i}||$. In the reciprocal space, the plane of diffraction are infinite line. So, in the case of a perfect crystal, with a perfect detector, the intersection with Ewald's sphere should be points. However, since the crystal may present some defects and neither the gun or the detector are perfect, the intersections appear as lines on the diffracted pattern.

The growth of QDs makes the surface rough at the scale of the length of coherence of the beam. The electrons can interact with more layers while passing through the dots. This can be seen on the diffraction pattern, where lines become points.

I.2 Self-assembled CdTe/ZnTe quantum dots doped with single Cr atoms

I.2.1 Substrate preparation

The samples were grown on ZnTe(100) substrates. Two cleaning methods were tested:

i) etching of the substrate in a Bromide solution (Br_2-C_2H_5OH)

ii) exposition of the substrate to a hydrogen radical plasma.

The etching process was done in four steps. All of them, except the etching in Bromide-ethanol, occured in an ultrasonic cleaning device vibrating the sample at 43 kHz for 3 minutes. We began with a cleaning in acetone, followed by one in ethanol. The third step was etching in Bromide-ethanol, with 3% of Bromide, for 1 minute. We rinsed the sample in methanol. Once rinsed, we keep the sample in ethanol until mounting them on the sample holder. The transfer from the ethanol to the MBE chamber takes a few minutes, and some contamination might occurs during this time.

In order to avoid contamination during the transfer, another type of cleaning of the surface was tried: using hydrogen radical (H^*) to remove the impurity at the surface. The substrate was rinsed four times, first in acetone, then ethanol and then water, for a duration of 5 min with sonication at 43 kHz, and finally 5 more minutes in water with sonication at 23 kHz. once the sample was clean, it was mounted on the sample holder and loaded in the MBE system. The hydrogen radicals were formed in a seperate chamber by a RF power source operating at 13.6 MHz and at a power of 300 W. The substrate is exposed to the plasma for 15 min at 400°C. The evolution of the surface was monitored with the RHEED: the diffraction pattern presented strikes after the exposition to H^* plasma.

Most of the sample we grew were done using the Br-ethanol etching. Cleaning by H^* radicals was tested later during my PhD, and only a few containing Cr-doped dots. In this thesis, the only sample presented cleaned with the later technique is the charge control sample.

I.2.2 Stranski-Krastanov quantum dots growth

The self-assembled dots are formed using Stranski-Krastanov growth. A material with a different lattice parameter than the substrate is deposited. This lattice parameter difference create strain in the grown layer. Growing over the critical thickness, the layer may relax in different fashion, depending on the material. In Stranski-Krastanov growth, the relaxation occur via the formation of island, the QDs, on the layer. QDs formed by this method are called Stranski-Krastanov dots (SK dots). For CdTe/ZnTe, the critical thickness is $h_c = 6.5$ MLs [2]. However, the dots does not form naturally in CdTe/ZnTe: if left as is, dislocation will form in the layer to relax the strains. In order to form the dots, a layer of amorphous Tellurite has to be deposited on the surface of the sample, and then evaporated [3].

The CdTe QDs layer is grown by Atome Layer Epitaxy (ALE), or Migration-Enhanced Epitaxy (MEE). While in classical use of MBE, the elements of the material are co-deposited on the substrate, in ALE, each cell is open one after the other, in sequence. Between each opening, the sample is left under vacuum in order to relax the surface. Such a growth is auto-regulated: when only one element is open, only a given quantity of material will be deposited and then the growth will stop until the other element is also deposited. The deposited quantity of material before the growth stop depends only on the substrate temperature. This allow for a really fine control of the growth and the deposited thickness is achieved. A full cycle correspond to opening each cell once.

Table I.1: Targeted flux in Beam Equivalent Pressure (BEP) for each cell during the growth of the strained QDs.

Elements	Targeted BEP (Pa)	Targeted flux (atoms.cm^{-2}.s^{-1})
Zn	9.1×10^{-5}	1.3×10^{14}
Te	6.0×10^{-5}	5.8×10^{13}
Cd	6.0×10^{-5}	6.7×10^{13}

The targeted flux chosen for the growth of the CdTe/ZnTe QDs are presented in Tab. I.1 for each cell used during the growth. These flux were measured via a Bayard-Alperd pressure gauge inside the MBE chamber, and are therefore given in

Beam Equivalent Pressure (BEP). It was shown that the best quality of ZnTe was achieved for a growth in excess of Zn [4]. Otherwise, vacancies appear in the bulk, optically visible, and the surface is rougher. The ZnTe barriers were therefore grown in excess of Zn.

The relative flux of the elements have no influence on the ALE process. We only have to be careful to deposit enough of each element to saturate the surface at each opening. We therefore chose to use the same flux for both Cd and Te [5].

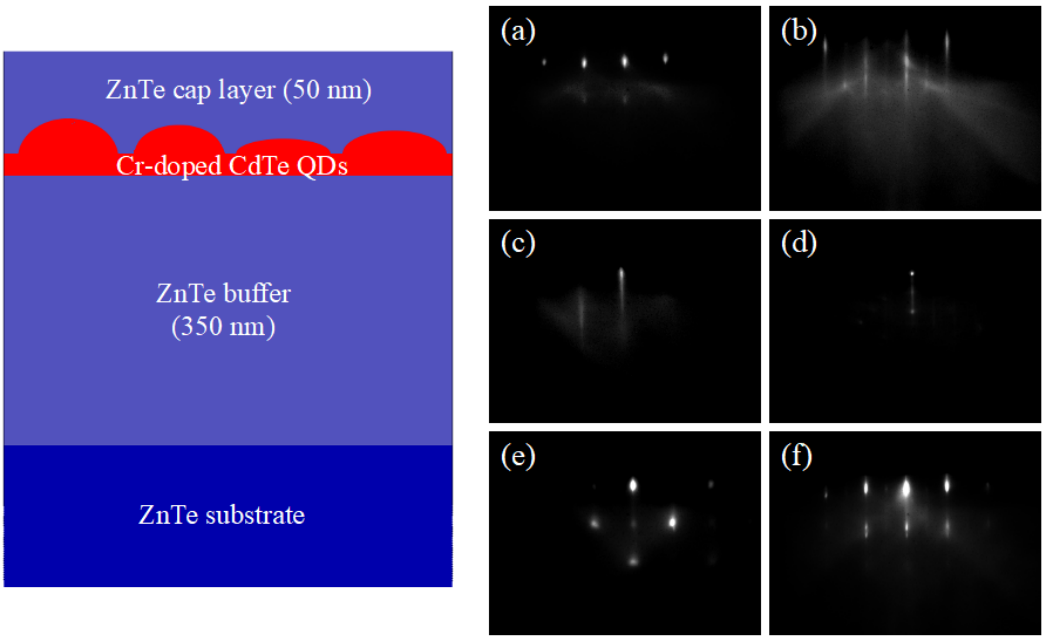

Figure I.3: Left: Layer structure of the strain Cr-doped CdTe QDs samples. Right: RHEED pattern taken along the Te reconstruction line at different key moment of the growth: (a) before the growth of the ZnTe buffer, (b) after the growth of the ZnTe buffer, (c) end of the (Cd,Cr)Te layer deposition, (d) after the Te deposition, (e) after the Te evaporation ($T_{substrate}$ = 163°C) and (f) after the growth of the ZnTe cap.

Beginning the growth, the substrate temperature was initially raised to 400°C. The Zn cell shutter was open starting at 355°C, in order to flatten the surface for the growth. While it took several minutes to raise the substrate temperature, the growth was stop by the auto-regulation of the ZnTe growth. When the substrate temperature reach 400°C, the Te shutter was also open, in order to grow the ZnTe buffer layer. This thick ZnTe layer keep us far from the substrate surface, that can have some default, and gives us a flat surface [6]. The surface quality is checked by RHEED, presenting clear diffraction lines (Fig. I.3 (b)). The substrate temperature

was then lowered to 295°C, the Zn cell being open until the temperature reach 355°C.

CdTe is grown by ALE, in which the choice of substrate temperature fix the quantity of material deposited at each cycle. It was found that 0.5 ML of CdTe is deposited at each cycle for a substrate temperature between 260°C and 290°C [5]. Taking a temperature between those two limits allows for a small uncertainty on the substrate temperature while keeping a really good control on the growth of the sample.

The growth during ALE was monitored via the intensity of the specular spot. Focusing on the lowest angle reflected spot, called the specular spot, one can see small variations in the reflected intensity during the growth. This is the same mechanism as the one presented in Fig. I.2 for the RHEED oscillation during the construction of the surface. Fig. I.4 presents oscillations taken during an ALE. Low intensity moments correspond to Cd deposition, high intensity to Te deposition. One can see series of low intensity, high intensity, medium intensity and high intensity repeating. Those corresponds to two ALE cycles, and therefore the growth of single CdTe monolayer [5]. We can also see the relaxation of a layer: the surface becomes then rougher, and the specular sport stays at low intensity.

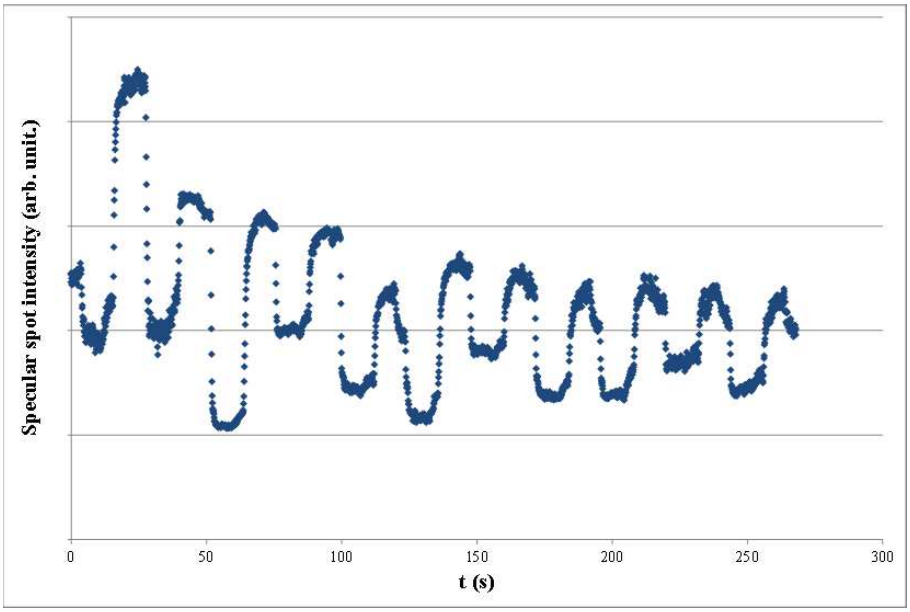

Figure I.4: RHEED oscillation for the ALE of the strained dots.

One of the main goal of this work was to calibrate the Cr flux in order to optimize the probability of having a single Cr atom in most of the QDs of the sample. A first guess is that the Cr density must be of the same order as the

QDs density at the surface of the sample. Supposing that all the Cr atoms get adsorbed on the sample, the quantity of deposited atoms is given by the flux of said atom times the time during which the cell stays open (exposition time). Due to the opening and closing time of the shutter, the exposition time cannot be shorter than a few seconds. Therefore a really small flux has to be chosen, with a BEP of the magnitude of 10^{-9} Pa, which is of the same order of magnitude than the main chamber pressure. It cannot therefore be not reliably measured using the gauge pressure. In order to find the cell temperature needed to reach such small flux, we used Arrhenius law, stating that the log of the flux of a cell varies linearly with the inverse of its temperature. From flux measured at higher temperature, we calculated the coefficients and deduced the aimed temperature of the Cr cell. The resulting curve is presented on Fig. I.5, with coefficients values. The optimisation was done starting with the know how acquired in Grenoble on the growth of CdTe/ZnTe QD dopes with single Mn and trying to optimise it for the Tsukuba machine, through a feedback loop with the micro-PL characterization in Grenoble.

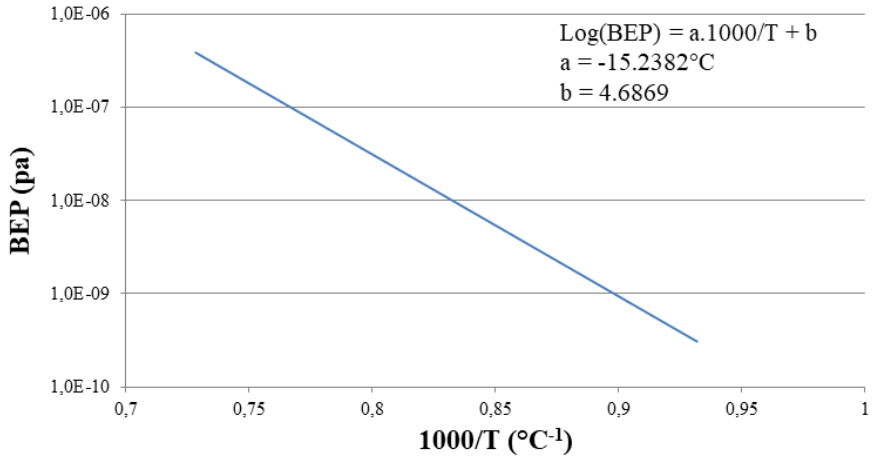

Figure I.5: Cr BEP as a function of 1000/T. Parameters of the Arrhenius law are given in the top left.

This really small flux was achieved by heating the Cr cell around 1000°C, and opening the cell only once during the deposition of the CdTe layer. In order to have QD emitting in the right range of wavelength for our optical setup (around $\lambda = 600$ nm), the optical CdTe thickness is 6.5 MLs. However, this is close to the critical thickness. Therefore, to diminish the risk of dislocation in the CdTe layer, some samples were grown with 5.5 MLs of CdTe. The Cr cells was opened when half of the CdTe layer was grown (7th cycle for the 6.5 MLs samples, 5th cycle for

the 5.5 MLs samples). The ALE sequences used to grow the CdTe layer is shown in Fig. I.6.

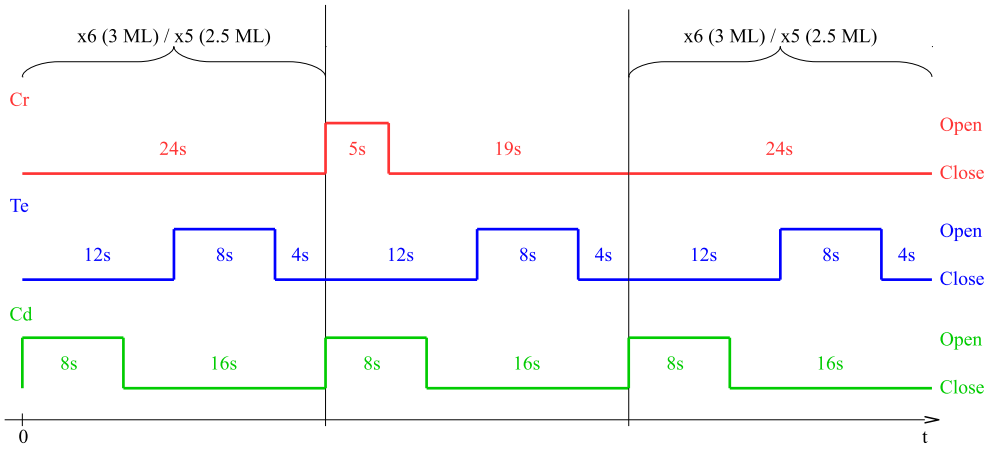

Figure I.6: Opening and closing cycles of each cells used to grow either 6.5 MLs or 5.5 MLs of (Cd,Cr)Te for the formation of Cr-doped SK dots.

After the growth of the CdTe layer, we lowered the substrate temperature to 210°C to deposit an amorphous Te layer. It was deposited during 5 minutes. We then heated up the substrate again to 320°C, were we stayed for 20s in order to evaporate all the deposited Te [7]. The formation of dots was confirmed by a spotty diffraction pattern like the one presented on Fig. I.3 (f). The Zn and Te cells were then opened, while the substrate temperature was raised to 350°C in order to grow a protective layer of about 50 nm of ZnTe above the QDs.

I.2.3 Optical characterization

The samples were studied in Grenoble, at the Neel Institute. The characterization of the samples was done in two steps. First, we took macro-photoluminescence spectra, on a large energy range, typically between 1.8 and 2.3 eV, with a laser set at 2.9 eV. This allow us to test the PL of the sample. As said in Sec. **??**, if the Cr concentration is too high, it may kill the PL of the dot layer, and thus it will not be seen in the macro-PL. If luminescence from the sample is seen in macro-PL, the sample is studied by micro-photoluminescence (μ-PL), on a much narrower energy band (about 10 meV), to study dots individually. A high refractive ($n \approx 2.5$) index hemi-spherical Solid Immersion Lens (SIL) was mounted on the sample before their study, to improve the spatial resolution and enhance the collection efficiency of a single dot photoluminescence (PL) in a low temperature optical microscope. The sample is scanned randomly. We judge the quality of the sample by the number

of actual dots we found with single Cr embedded inside, and by the proportion of thin emission peaks (a few tens of μeV) versus broad ones (in the meV range): if we saw mainly broad peaks, it suggests that the Cr concentration is too high.

Table I.2: List of samples where single dots with single Cr was found.

Sample name	Cleaning process	# CdTe MLs	Targeted Cr concentration (%)	# Cr-doped dots found
dot334	Br etching	6.5	0.09	3
dot338	Br etching	6.5	0.05	2
dot359	Br etching	6.5	0.11	1
dot363	Br etching	6.5	0.21	2

The samples where QDs doped with a single Cr atom were found are listed in Tab. I.2. The Cr concentration in the sample was estimated using the Cr flux. The Cr composition is given as percentage of the cation site occupancy ($Cd_{1-x}Cr_xTe$). We see that correct samples were found for a large range of concentration. The probability to find good Cr-doped dots in dot338 and dot363 is about the same. However, dot363, with the higher Cr targeted concentration, presents a lot of broad peaks. All samples grown with a Cr concentration higher than 0.20% had a luminescence too weak to be studied properly. We can estimate that the good range of concentration is between 0.05% and 0.20%. Some more test have to be done in order to fine tune the Cr composition.

I.3 Charge tunable samples and strain-free samples

I.3.1 Charge tunable samples

The charge control samples are grown in order to be able to apply an electric field on the dot layer. The growth occurs on a p-doped ZnTe substrate. It gives the sample a conductive back. The growth was done in order to form Stranski-Krastanov dots, as described in the previous section. All the charge tunable samples were clean using H^* plasma. Thinner buffer and cap layers were necessary in order to be able to apply a stronger electric field on the dot layer. We chose thicknesses between 150 nm and 200 nm for the buffer, and of 110 nm for the cap.

The conductive surface was formed by a thin, semi-transparent gold layer, forming a Schottky junction with the sample cap layer. It was deposited by sputtering just after the MBE growth in order to keep a clean surface. The samples were kept in nitrogen atmosphere during the transport between the MBE and the sputtering

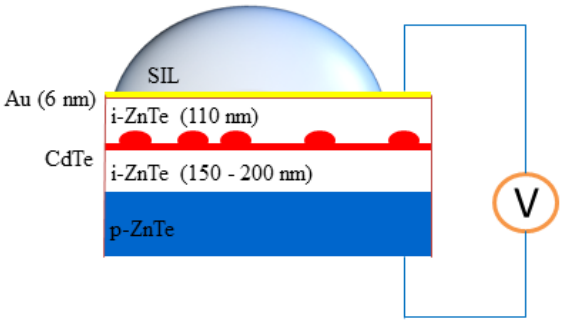

Figure I.7: Schema of the charge control structure, on a p-doped ZnTe substrate and with a thin, semi-transparent gold layer deposited on the surface.

machine. A deposition time of 35 s was chosen. Fig. I.7 shows a schema of the sample as it was studied.

Only one Cr-doped charge tunable sample was grown and studied during this PhD, named dot390. It was decided to make the CdTe layer 5.5 MLs thick in order to not have dislocation in the QD layer. The targeted Cr concentration was 0.16%.

Optical characterization

In order to test the application of bias voltage in the sample, we glued two electrodes with silver lacquer. A SIL was mounted on top of the sample. We looked at the PL of single dots and see their evolution under the application of a bias voltage. Fig. I.8 (a) presents the results of such an experiment.

The main result of the experiment is the appearance of different excitonic species depending on the applied electric field. The spectrum are dominated by the neutral state of the quantum dot for an applied electric field of V = -1.5 V (Fig. I.8 (c)). At this voltage, the neutral excitonic species X and X^2 are the strongest. Charged excitons still appear because of charge variations occuring close to the QD, injecting electron or holes inside it. Further lowering the bias voltage, the probability of the dot to be negatively charged increases. Neutral excitonic species disappear and the peaks of the negatively charged species (X^-, X^{--} and X_2^-) become dominant. A spectra taken at V = -8 V is presented on Fig. I.8 (d). One can notice that, X^{--} is splitted into two group of two peaks, around 1917.5 meV and 1933 meV on Fig. I.8 (d). It is caused by the electron-electron interaction and has already been observed in InAs quantum dots [9]. On the contrary, applying a positive bias voltage increases the probability to detect positively charged exciton complexes, maximizing X^+ and X^{++} intensity. This is shown on Fig. I.8 (b) for a bias voltage of V = +3 V. This shows that we can select efficiently the charge of a quantum dot applying a bias voltage across it.

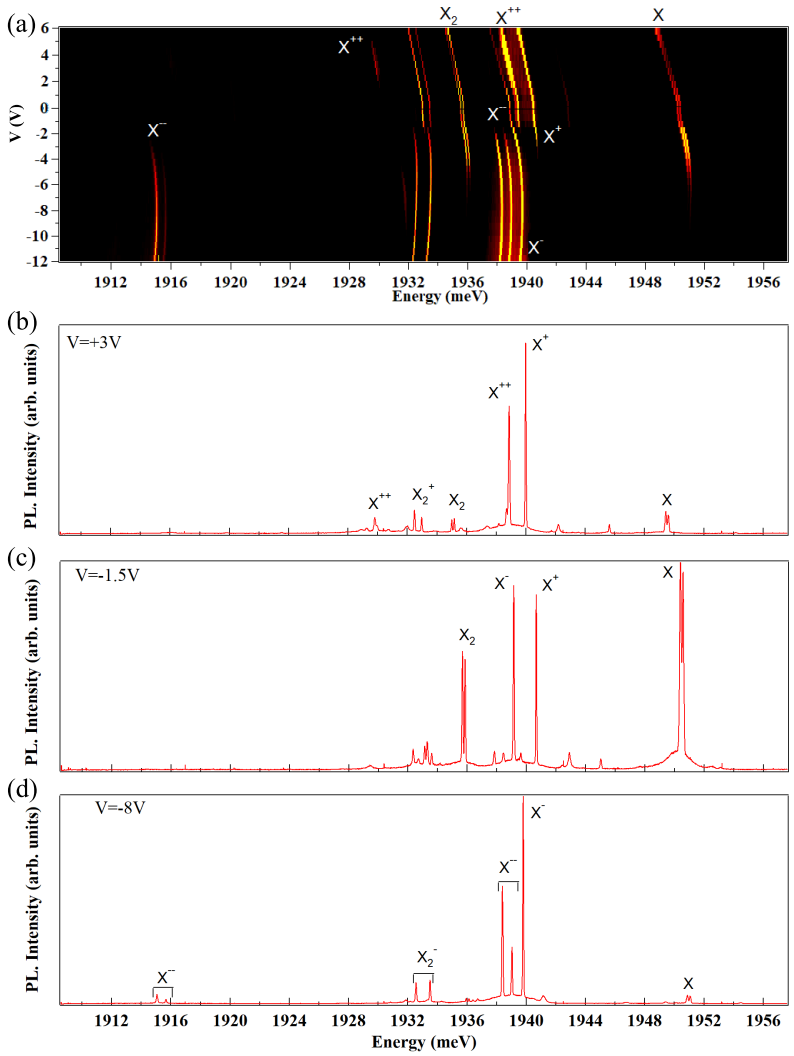

Figure I.8: (a) Evolution of the PL of a single dot under application of a bias voltage V. Below are presented spectra of the dot taken under three different values of bias voltages: (b) V = +3 V (positively charged), (c) V = −1.5 V (neutral) and (d) V = −8 V (negatively charged). Identification of the different species was done following ref. [8].

dot390 was studied under μ-PL. However, no Cr doped quantum dots were found. Some dots looking like dots doped with a single Cr atom were found, but further investigation shows no sign of magnetic atom in them. Such QDs are discussed in more details in Sec. **??**.

I.3.2 Strain-free quantum dots

In SK dots, the some strain remain in the QD layer, and we have no control on them. As will be discussed later, remaining strains limits the life-time of the Cr spin. We decided therefore to grow strain-free dot to get rid of those limits. They are formed by the thickness fluctuations of a CdTe quantum well in $Cd_{0.7}Mg_{0.3}Te$ barriers, grown on a CdTe substrate. These fluctuations form steps localizing the carriers, acting as QDs. We chose to use $Cd_{0.7}Mg_{0.3}Te$ to keep a lattice parameter close enough to CdTe to grow thick enough barriers, and keeping enough gap difference to localize the carriers. The needed flux for this growth are shown in Tab. I.3.

Table I.3: Aimed flux for each cell during the growth of the strained samples.

Elements	Targeted BEP (Pa)	Targeted flux (atoms.cm^{-2}.s^{-1})
Cd	6.0×10^{-5}	6.7×10^{13}
Mg	2.1×10^{-6}	4.7×10^{12}
Te	7.0×10^{-7}	5.8×10^{13}

The critical thickness of $Cd_{0.7}Mg_{0.3}Te$ on CdTe is not exactly known. Systematic studies were done on CdTe/CdZnTe gives an empirical law to calculate the critical thickness [10]. This law was used for different II-VI material and gives a good approximation of the different critical thickness, overestimating slightly the effects of strain. For CdTe/$Cd_{0.7}Mg_{0.3}Te$, we found a critical thickness $h_c = 130$ nm. We chose to grow 40 nm below the QW, and 90 nm above it, to keep the surface far from the quantum well.

The strain-free sample were grown on a hybrid substrate formed by a thick CdTe layer grown on GaAs. It was done on a fourth of a 2 inches GaAs substrate and protected by Te. The GaAs substrate was cleaned using H* plasma. A thin layer (about 7 nm) of ZnTe was first grown at 415°C in order to get the right crystal orientation when growing the CdTe layer. We then grew a CdTe layer of about 3 μm at 360°C, to recover a good crystallinity of the CdTe layer [11]. The RHEED taken after the growth of the CdTe layer (Fig. I.9 (d)) shows sharp straight line, showing the recovery of a flat surface.

For the growth of strain free samples, we began to heat the substrate temperature to 300°C and waited a few seconds to remove all the deposited Te; We then heated the sample to 360°C. Starting at 320°C, we opened the Te cells in order to stabilize the surface. When the substrate temperature was stabilized at 360°C, we opened the Cd cells and grew a 2.35 μm of CdTe on top of the 3 μm grown on the hybrid substrate, in order to be get far from the surface that might have been

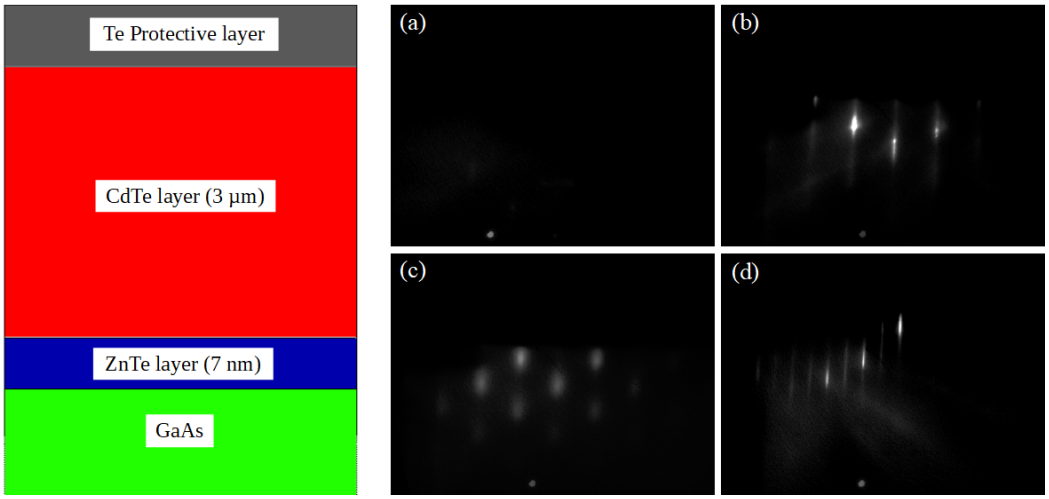

Figure I.9: Left: Layer structure of the hybrid substrate with its protective Te cap. Right: RHEED pattern taken at different key moment of the growth: (a) before H^* cleaning of GaAs, (b) after H^* cleaning of GaAs, (c) after the growth of the ZnTe layer, (d) after the growth of the CdTe layer.

slightly damage during the conservation or the Te evaporation.

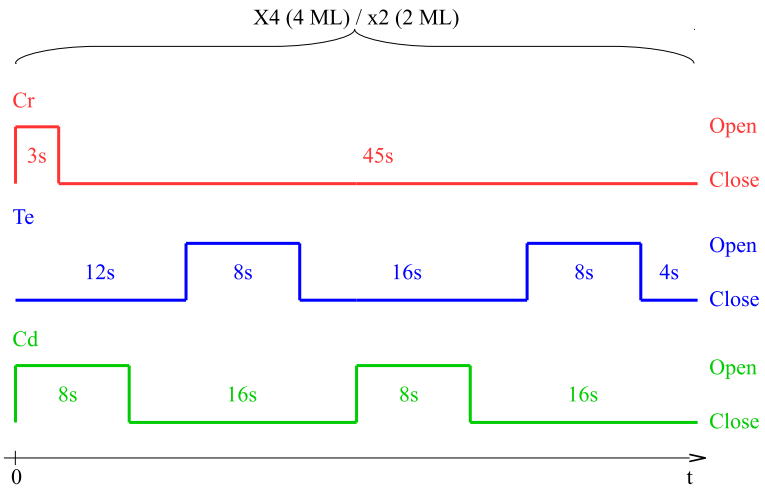

Figure I.10: Opening and closing cycles of each cell for the ALE of strain free (Cd,Cr)Te samples.

We grew the 40 nm $Cd_{0.7}Mg_{0.3}Te$ barrier on this buffer layer. Once the done, we lowered the substrate temperature under Te flux, in order to smoothen the

sample surface. Once the substrate temperature reach 295°C, we began the ALE of the QW. Two QW thicknesses were tested: 4 ML and 2 ML. The Cd and Te cycles were the same as for the SK dots. The Cr, however, was open for only 3 s, but once every two cycles, for a total of 4 opening in the 4 ML case, and 2 opening for the 2 ML case. The whole recipe is described in Fig. I.10.

We then raised the substrate temperature up to 360°C, under a Te flux, in order to proceed to the growth of the upper barrier, acting also as a protective layer. The opening time was there calculated to grow 90 nm of $Cd_{0.7}Mg_{0.3}Te$.

Optical characterization

Four samples of strain-free dots doped with Cr were produced (see Tab. I.4). The Cr concentration were taken high because it was see on the strain-free dots grown in Grenoble that a higher concentration of Mn was needed in strain-free dots than in SK dots. It was supposed to be the same with Cr. The Cr concentration was later rose after no dot doped with a single Cr was found.

Table I.4: Strain-free QDs doped with Cr.

Sample	# CdTe MLs	Cr aimed concentration (%)	Probability of Cr-doped QD
SFD4	4	0.35	None found
SFD5	2	0.15	None found
SFD6	2	0.54	None found
SFD7	2	0.35	None found
SFD8	2	0.75	None found

The sample presented thin and intense peaks, as shown in Fig. I.11. It hints at a better confinement of the carriers in the QDs than the strain-free dots grown in Grenoble. This may be caused by higher steps than expected at the $CdTe/Cd_{0.7}Mg_{0.3}Te$ interface.

As discussed in Sec. **??**, the presence of a magnetic atom splits the emission of the exciton into several peaks, the number depending on the spin of the magnetic atom. Such complex was not found in the strain-free samples. This may be caused by a problem in the Cr incorporation. The Cr possibly is not well embedded in the QW layer. More tests have to be done, depositing the Cr at different moment of the growth.

Another possible cause of this absence could lie in the absence of strain. In SK dots, the presence of strains increases the probability of the Jahn-Teller deformation to occur along the z axis. In strain-free dots, all direction are equivalent,

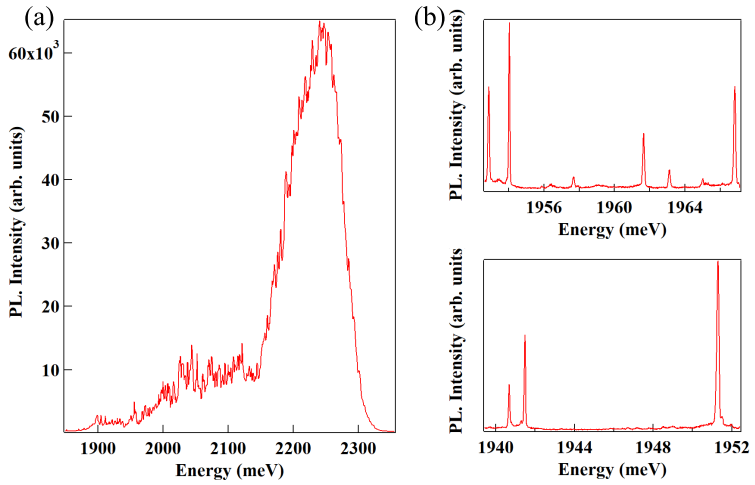

Figure I.11: (a) Macro-PL of a SFD5. (b) Examples of spectra taken under μ-PL in SFD5.

and we expect two third of the Cr-doped dots to be undetectable because they are quantized in the plane, creating no splitting visible in our setup.

In order to increase the probability for the Cr to be quantized along the z axis, it is proposed to slightly strain the quantum well. This might be done by growing the sample on $Cd_{0.96}Zn_{0.04}Te$ instead of CdTe. The lattice parameter of Cdte and $Cd_{0.96}Zn_{0.04}Te$ have a lattice mismatch of only 0.3%, so the strain it will create in the lattice should remain weak. They should however be enough to increase the probability of a deformation along the z axis, making more dots visible in our setup.

Conclusion

We saw in this chapter how we grew the samples studied in the next chapters. The samples were characterized in Grenoble. SK dots with single Cr atom embedded were found and studied. New Cr concentration were tested in Tsukuba after the feedbacks from Grenoble. More tests have to be done to increase the probability of finding dots doped with a single Cr atom.

First step toward new kind of sample were also done: strain-free QD with single Cr, and SK dots with single Cr embedded in a field effect structure. Localized carrier emission was detected in the former, and we successfully applied bias voltage on the later. However, for both, no Cr-doped dots were found in. More tests have to be done to optimize their growth.

Bibliography

[1] A. Cho and J. Arthur, "Molecular beam epitaxy", Progress in Solid State Chemistry **10**, 157–191 (1975).

[2] J. Cibert, Y. Gobil, L. S. Dang, S. Tatarenko, G. Feuillet, P. H. Jouneau, and K. Saminadayar, "Critical thickness in epitaxial CdTe/ZnTe", Applied Physics Letters **56**, 292–294 (1990).

[3] F. Tinjod, B. Gilles, S. Moehl, K. Kheng, and H. Mariette, "II–VI quantum dot formation induced by surface energy change of a strained layer", Applied Physics Letters **82**, 4340–4342 (2003).

[4] R. D. Feldman, R. F. Austin, P. M. Bridenbaugh, A. M. Johnson, W. M. Simpson, B. A. Wilson, and C. E. Bonner, "Effects of Zn to Te ratio on the molecular-beam epitaxial growth of ZnTe on GaAs", Journal of Applied Physics **64**, 1191–1195 (1988).

[5] J. M. Hartmann, G. Feuillet, M. Charleux, and H. Mariette, "Atomic layer epitaxy of CdTe and MnTe", Journal of Applied Physics **79**, 3035–3041 (1996).

[6] J. H. Chang, M. W. Cho, H. M. Wang, H. Wenisch, T. Hanada, T. Yao, K. Sato, and O. Oda, "Structural and optical properties of high-quality ZnTe homoepitaxial layers", Applied Physics Letters **77**, 1256–1258 (2000).

[7] P. Wojnar, C. Bougerol, E. Bellet-Amalric, L. Besombes, H. Mariette, and H. Boukari, "Towards vertical coupling of CdTe/ZnTe quantum dots formed by a high temperature tellurium induced process", Journal of Crystal Growth **335**, 28–30 (2011).

[8] Y. Léger, L. Besombes, J. Fernández-Rossier, L. Maingault, and H. Mariette, "Electrical control of a single mn atom in a quantum dot", Phys. Rev. Lett. **97**, 107401 (2006).

[9] M. Ediger, G. Bester, B. D. Gerardot, A. Badolato, P. M. Petroff, K. Karrai, A. Zunger, and R. J. Warburton, "Fine structure of negatively and positively charged excitons in semiconductor quantum dots: electron-hole asymmetry", Phys. Rev. Lett. **98**, 036808 (2007).

[10] J. Cibert, R. André, C. Deshayes, G. Feuillet, P. Jouneau, L. S. Dang, R. Mallard, A. Nahmani, K. Saminadayar, and S. Tatarenko, "CdTe/ZnTe: critical thickness and coherent heterostructures", Superlattices and Microstructures **9**, 271–274 (1991).

[11] K. Shigenaka, L. Sugiura, F. Nakata, and K. Hirahara, "Lattice relaxation in large mismatch systems of (111)CdTe/(100)GaAs and (133)CdTe/(211)GaAs layers", Journal of Crystal Growth **145**, 376–381 (1994).